El Niño Hindcast with a Simple Dynamical Model

Sophia T. Merrifield
Department of Physics, Yale University, New Haven, CT 06520

Advisor: Professor Alexey V. Fedorov
Department of Geology and Geophysics

The El Niño Southern Oscillation (ENSO) is a coupled ocean and atmospheric phenomenon that has vast implications for weather and climate globally. Responsible for droughts and heavy flooding events, ENSO variability is important to the issue of climate change and its societal impacts. Our ability to understand this climate phenomenon and predict El Niño is crucial to climate prediction on regional and global scales. While comprehensive climate models have made significant progress in El Niño prediction during the last decade or so, the reliability of their forecast remains relatively low even on seasonal timescales. For example, predictions made today for sea surface temperatures in the eastern equatorial Pacific with a 6-month lag by different models may differ by 2^oC.

In this work, we explore a recently developed simple dynamical model of ENSO for prediction (or more precisely for hindcasting past El Niño events). The model is derived assuming that El Niño is a relatively low-frequency phenomenon as compared to fast timescales associated with equatorial wave propagation. As the first step, we have introduced nonlinearities to the governing equations of the model and examined their effects. Next, we use tuning parameters to strengthen the skill of the model. For example, α, the wind stress curl parameter, controls the extent of wind anomalies near the equator. The developed model exhibits reasonable predictive skill as seen in the correlation with the observations and its RMS error.

I. INTRODUCTION

The El Niño-Southern Oscillation (ENSO) is defined by warming and cooling patterns in surface waters in the eastern tropical pacific ocean. The southern oscillation refers to an atmospheric contribution due to surface pressure gradients in the western tropical pacific. El Niño is characterized by a flow of warm water on the eastern side of the pacific due to weakened zonal winds which flatten the thermocline and consequently cause warm sea surface temperature (SST) anomalies. La Niña, instead, is characterized by strong zonal winds causing storage of warm water in the west, steepening the thermocline and allowing cold water to surface in the east. The important component of this phenomenon is the meridional (along longitude) mass distribution. Typical periods of El Niño range from 3-7 years.

Although variations in SST are localized in the equatorial pacific, ENSO events have implications on global climate. El Niño events have caused elevated rainfall in the Southern U.S. and Peru. Droughts in the Western Pacific and brush fires in Australia are other examples of ENSO's effects. In El Niño years, winter temperatures are warmer than normal in the northern central states and colder than usual in the Southeast and Southwest Biological effects on food chain are also observed, warm El Niño events can cause decline in productivity even reaching commercial fisheries. Although La Niña events are less intense in terms of SST anomalies, global impacts are still notable. In winter, for example, temperatures are relatively warmer in the Southeast and colder on average in the Northwest of the U.S. during a La Niña.

A climate feedback is a mechanism which amplifies (positive) or damps (negative) the effects of a change in climate forcing. Three climate feedbacks are notable in ENSO dynamics: thermocline, upwelling, and zonal advection. To illustrate these feedbacks Figure 2 assumes a warm SST anomaly which induces wind-stress anomalies. The thermocline feedback occurs when wind stress anomalies vary the slope of the thermocline causing an increase in the SST anomaly. Here we assume constant background upwelling. If, instead, we assume a background stably stratified temperature field the upwelling feedback leads to changes in upwelling which also increase the SST anomaly. The third feedback, zonal advection, occurs when the wind anomaly causes stronger zonal advection, under conditions where the annual-mean zonal SST gradient is negative, will cause an increase in the SST anomaly. [1]

Low frequency processes are integral to the under-

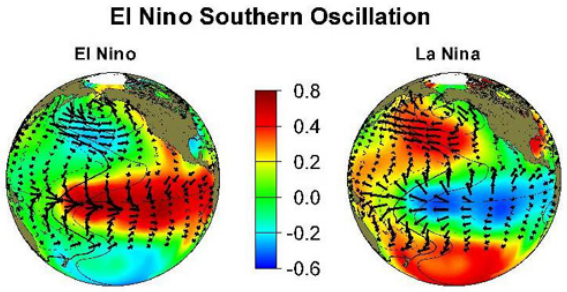

FIG. 1: Averaged temperature anomalies in ^oC in the equatorial pacific. Black quivers indicate intensity and direction of winds. An El Niño (La Niña) event is characterized by a $+.5^oC$ ($-.5^oC$) sea surface temperature anomaly. Strong El Niño events have reached 4^oC while La Niña events are generally weaker and are maximized at approximately -2^oC.

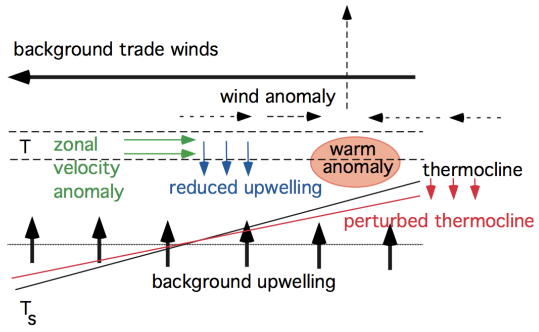

FIG. 2: A diagram of feedbacks to a warm anomaly associated with El Niño. Upwelling is reduced and the thermocline flattens.

standing of ENSO events. Coupling between low frequency wind variations and the ocean's response is fundamental to the dynamics of ENSO. Because it is a relatively slow process, we consider ENSO's small frequency of oscillation in comparison with the faster timescale of Kelvin and Rossby wave propagation. Kelvin waves have characteristic periods of 30-90 days. SST sensitivity to increases in equatorial upwelling or the slope of the thermocline is on the order of a few months. We therefore integrate the high frequency processes hoping to understand large scale net adjustments of the ocean. [2]

Ocean memory in other approximations, such as the original fast-wave limit [3, 4], neglect the adjustment time of the ocean thermocline, while in this study we account for it. By incorporating ocean memory into this work we encompass the dynamics of the ocean recharge and discharge oscillator.

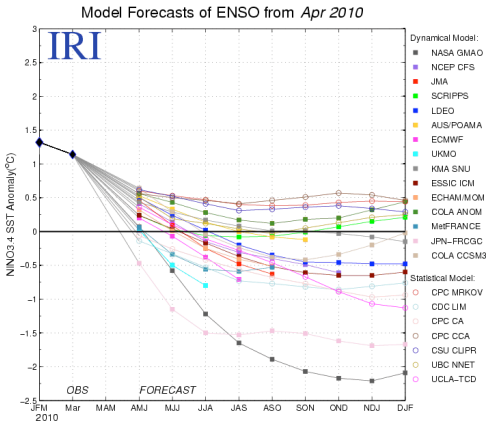

FIG. 3: Current operational models forecasting ENSO. Both dynamical and statistical models are shown. The variance in the predictions of these models shows the need for more rigorous models of ENSO dynamics.

The motivation for this work comes from the large variability (Fig. 3) in operational models at present. We propose a relatively efficient model that in one equation for temperature evolution can encapsulate the fundamental dynamics of ENSO.

II. METHODOLOGY

To represent ENSO we use the long-wave approximation on the equatorial β-plane and begin with the linear reduced-gravity shallow-water equations.[5]

$$u_t + g'h_z - \beta y v = \tau/\rho D - \epsilon_m u \quad (1)$$

$$g'h_y + \beta y u = 0 \quad (2)$$

$$h_t + H(u_x + v_y) = -\epsilon_m h \quad (3)$$

u=u(x,y,t) [zonal current]
v=v(x,y,t) [meridional current]
H - the mean depth of the thermocline
h=h(x,y,t) - thermocline depth anomalies
τ=τ(x,y,t) - the zonal components of the wind stress
ρ - mean water density, ($\Delta\rho$ - the difference between the density of the upper (warm) layer and the density of the deep lower layer)
g=g($\Delta\rho/\rho$) - the reduced gravity
D is the nominal depth characterizing the effect of surface winds on the ocean thermocline (frequently it is assumed that D=H).

Simple Rayleigh friction in the momentum equations and a linear parameterization of water entrainment at the base of the mixed layer in the continuity equation are incorporated in ϵ_m, the oceanic damping rate.[2] We non-dimensionalize as follows:

$$x- > xL, \qquad u- > uc_k, \qquad v- > \frac{vc_kL_R}{L},$$

$$h- > hH, \qquad x- > xL, \qquad y- > yL_R$$

$$t- > \frac{tL_R}{c_k}, \qquad \tau- > \frac{\tau\rho c_k^2 D}{L}, \qquad \epsilon_m- > \frac{\epsilon_m c_k}{L_R}$$

L - basin width L_R - equatorial Rossby radius of deformation

$$L_R = \sqrt{\frac{c}{\beta}}, \qquad c = \sqrt{(gH)} \quad (4)$$

is the phase velocity of linear baroclinic Kelvin waves, and time is scaled using the basin crossing time for the Kelvin wave,

$$T_k = \frac{L_R}{c_k} \quad (5)$$

Some typical values for the tropical Pacific ocean are ($\Delta\rho/\rho$=0.006; L=150^o, H=120m; D=80m;

$$c_k = 2.7m/s, \qquad L_R = 340km;$$
$$T_k = 2.4months; \qquad \epsilon_m = 2.01/years$$

The primary data used in this model is NINO3

temperature anomalies from the Kaplan dataset (http://iridl.ldeo.columbia.edu/SOURCES/.KAPLAN/). Following the method of Fedorov (2010) [2] we arrive at the sea surface temperature equation

$$\frac{d}{dt}T_e + (\epsilon_w + \epsilon_T)T_e = \epsilon_w \frac{h_e}{\Delta} \tag{6}$$

Another way of writing this relation is

$$\frac{d}{dt}T_e + aT_e = b\int e^{-\epsilon_m t'} I(\alpha, t')T_e(t-t')dt' \tag{7}$$

where

$$a = \epsilon_w + \epsilon_T - (r + \frac{q}{\sqrt{x_c}})\epsilon_h; \qquad b = \frac{q\epsilon_h}{\pi\sqrt{x_c}} \tag{8}$$

Here, T_e is the sea surface temperature in the eastern equatorial pacific, ϵ_m is the ocean damping timescale. h_e describes the depth of the thermocline in the eastern equatorial pacific. ϵ_T is thermal damping and x_c is the location of the maximum of wind stress anomalies.The terms r and q are coefficients for different lengths of the averaging integral in the eastern Pacific.

$$\epsilon_h = \tau_o \frac{\epsilon_w}{\Delta} = \gamma_o \frac{w_e \tau_o}{d\Delta} \tag{9}$$

This parameter describes the coupling between SST anomalies and the thermocline. w_e is the vertical upwelling velocity. Also defined is the function I in the convolution term,

$$I(\hat{\alpha}, t) = -\hat{\alpha}\int_0^1 e^{-\hat{\alpha}ts}\sqrt{\frac{s}{1-s}}ds \tag{10}$$

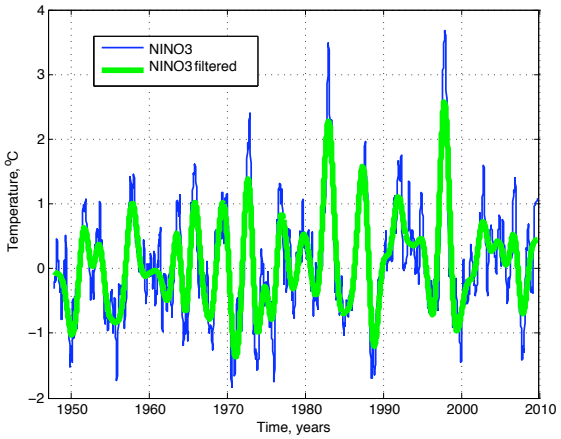

FIG. 4: The blue curve is the NINO3 index and the green curve represents filtered NINO3 data. To optimize our model we remove high frequencies from the input using a low-pass filter that removes periods shorter than 2 years.

The convolution on the right hand side of equation 7 describes the delayed thermocline response to variations in sea surface temperature (T_e). We do not account for Rossby or Kelvin waves as they are high frequency events in this context. Instead, we incorporate ocean memory that will have a net effect on the the current temperature. We choose 10-12 years of memory as it incorporates at least 1 ENSO event and most likely 2-3 recalling that the period of ENSO is between 3-7 years. Because our model is low frequency, we use a filtered version of the NINO3 data which removes high frequencies.

We will begin with a simple model that produces a damped oscillation of approximately 3 years (periodicity of ENSO).

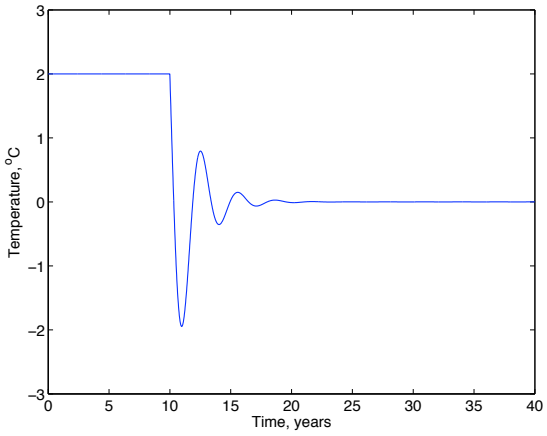

FIG. 5: The first ten years of the model are a convolution for ocean memory. In this figure, we use a constant temperature for illustrative purposes. At each NINO3 temperature point we output a damped oscillatory prediction like this one.

Four parameters are varied within physical bounds to improve the predictive skill of our model. Wind stress (τ_0), wind stress curl (α), the nondimensional vertical length scale over which the subsurface temperature changes by 1^oC (Δ), and the ocean damping rate (ϵ_m) are all varied relative to one another for the optimal set of parameters. High values of alpha increase the frequency of the model while lower values of delta increase the amplitude. Physically, increasing α means that wind anomalies are confined closer to the equator. A higher ocean damping rate, ϵ_m, will give stronger decay rates and longer oscillation periods. Δ, gives a measure of the thickness of the tropical thermocline.

We also wrote a second model based on the coupled system of equations:

$$\frac{d}{dt}T_e + aT_e = bW \tag{11}$$

$$\frac{d}{dt}W = -cT_e \tag{12}$$

$$a = \epsilon_w + \epsilon_T - (r + \frac{q}{\sqrt{x_c}})\epsilon_h; b = \frac{q\epsilon_h}{\pi\sqrt{x_c}}; c = \frac{\pi\alpha}{2x_c}$$

In this case the left side of equation 11 is an estimate of the integral given on the right side of equation 7. By approximating the ocean response term, the system simplifies and we can impose initial conditions in two ways. First, we can set the initial temperature and an approximate slope of the derivative using 2 or 3 points prior to the initial time. Secondly, we can impose, again, an initial temperature and an initial W.

The final method that we used to improve the skill of our model was by adding nonlinearities to the governing equations. This process will be more rigorously addressed in the future work section. The idea behind this method is to introduce nonlinearities to better represent certain relationships. ENSO, inherently, is a nonlinear process as La Niña events are uniformly weaker than El Niño events in intensity. An example of a simple quadratic nonlinearity is given

$$\frac{d}{dt}T_e = (...) + kT_e^2 \tag{13}$$

where k is a coefficient that we determine empirically.

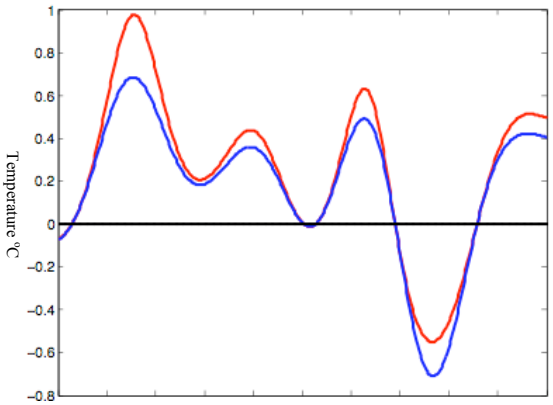

FIG. 6: In this plot we show for an arbitrary time step, we can add a quadratic nonlinearity to our temperature evolution equation and capture the asymmetry that exists between El Niño and La Niña. Here, the red curve has a nonlinearity and the blue curve does not.

By creating individual predictions from every NINO3 temperature point, we can create a hindcast of these predictions. We choose a specific length of prediction, e.g. 6 months, and choose the 6 month forecast from each prediction in the hindcast. We then have an array of 6 month predictions which we can analyze in relation to the NINO3 data at the corresponding time.

III. RESULTS

In this work we tried many different model variations with a range of results. Fig. 8 is a table summarizing these results. We define the skill of the model relative

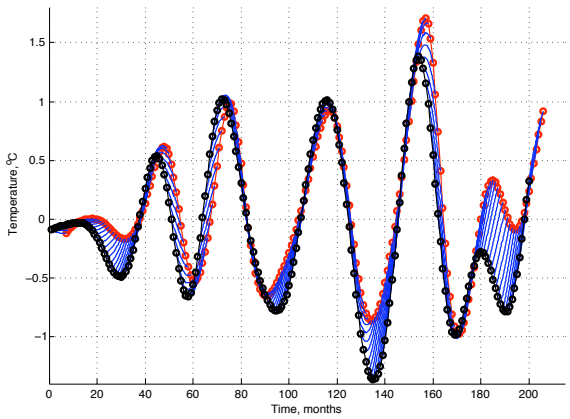

FIG. 7: The black points are NINO3 temperature points. The blue lines are predictions taken from each NINO3 temperature point. Creating a time series of these predictions, we can take the 6 month points (in red) and create a forecast 6 months into the future. Since this is a hindcast, we can then compare this 6 month forecast with the NINO3 index at the corresponding time.

to values of persistence. Persistence, in this sense, refers to the persistence of an initial anomaly moving forward in time. We consider the failures of the model just as valuable as the successes which we have quantified in the table below. What we have found, empirically, is that

Model	Correlation at 6 months
2 ODE's	~.45
Convolution	~.55
Filtered Convolution	~.85
Persistence (unfiltered)	.38
Persistence (filtered)	.66

FIG. 8: This table gives approximate results for each of our model runs. We choose to pursue the filtered convolution method, which has correlations at 6 months as high as .85.

we need an input that is low-frequency in order for the model to output strongly correlated forecasts. To implement this, we ran a low-pass filter on the NINO3 data to eliminate periods smaller than 2 years (Fig. 4). For a 6 month forecast we find significant predictive skill.

We are the only low-frequency model at present making it complicated to compare our results directly to other models. Instead, we quantify our skill by a correlation coefficient and an RMS error so as to account for shape and amplitude matching. We compare our results to persistence, a standard comparison in model diagnostics.

IV. CONCLUSIONS AND FUTURE WORK

In conclusion, we have developed a simple model that is computationally efficient and encapsulates the funda-

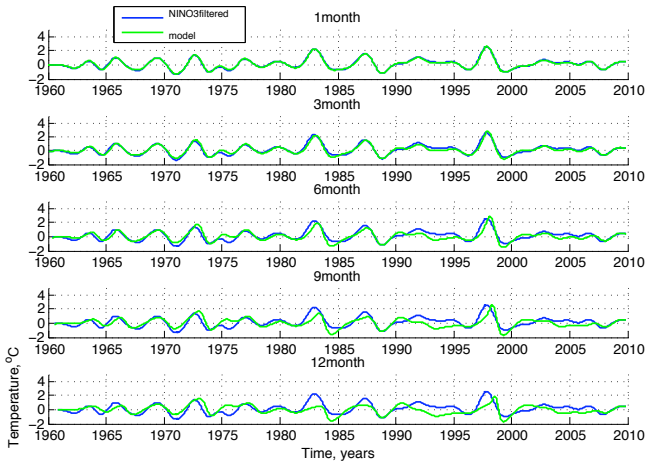

FIG. 9: For different lead times we create hindcasts to show the predictive skill of our model. Even at a 1 year prediction our model still exhibits notable skill.

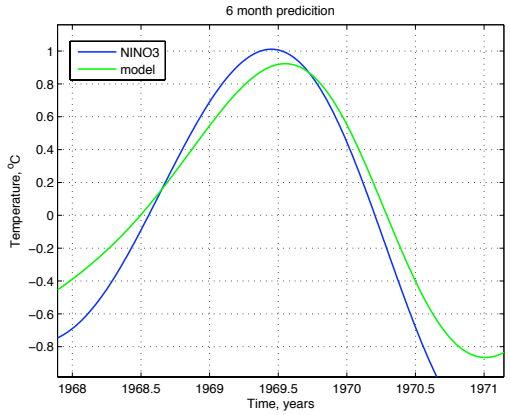

FIG. 10: This is a closer view of one of the El Niño events that we are forecasting at a 6 month lead. We are able to match shape and amplitude of the anomaly.

mental dynamics of ENSO. We are able to make 1 year forecasts that are significantly better than persistence and that may fall well below the typical variance between operational models and actual data.

There are two main areas of future work that I would like to propose. First, our model is efficient and therefore it is possible to give a more careful treatment to the ocean and atmospheric physics. By this I mean that we have made approximations in our governing equations and parameterizations that we may be able to more rigorously represent using, for example, nonlinearities.

The goal of this work is to develop an operational model which would mean reworking the input so that it would run with unfiltered NINO3 data. In order to do this we are in the process of developing a back filter, or a mechanism for filtering the input NINO3 data that does not use future time. At this stage we are exploring

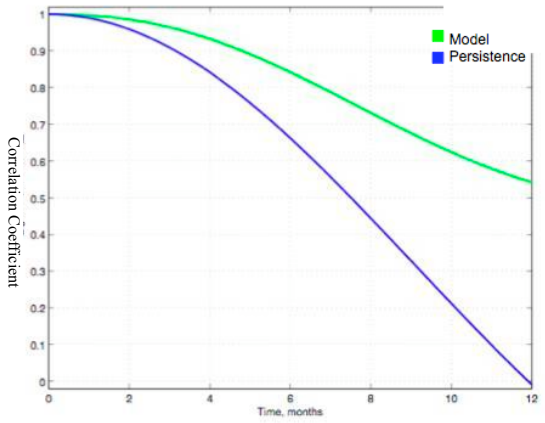

FIG. 11: The blue line represents persistence and our model is in green. For a one year forecast we are well above persistence.

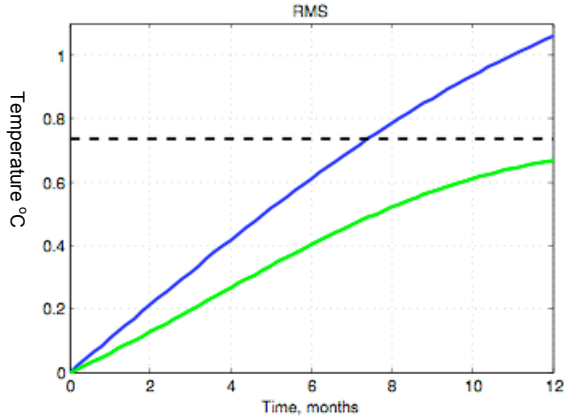

FIG. 12: The black dotted line represents the standard deviation of the NINO3 index. Blue is again persistence and green is our model plotted over a 1 year prediction. Our RMS error is well below persistence and simultaneously below the standard deviation as well.

two options. One, to run a low-pass filter that already exists in matlab on only previous times. The limitation with this is that filters are known to have trouble at the edges of data sets which may influence our convolution significantly. And secondly, we are trying to develop a theoretical approach to rework the convolution term so that it will filter the data in the integral. This work is in progress and seems promising.

[1] Henk A. Dijkstra. *Dynamical Oceanography*. Springer, 2008.

[2] A. V. Fedorov. Ocean response to wind variations, warm

water volume, and simple models of enso in the low-frequency approximation. *accepted to J. of Climate*, 2010.

[3] J.D. Neelin. The slow sea surface temperature mode and the fast-wave limit - analytic theory for tropical interannual oscillations and experiments in a hybrid coupled model. *J. Atmos. Sci. 48, 584-606.*, 1991.

[4] Z. Hao, J. D. Neelin, and F. F. Jin. Nonlinear tropical air-sea interaction in the fast-wave limit. *J. Climate 6, 1523-1544*, 1993.

[5] M.A. Cane and E. S. Sarachik. The response of a linear baroclinic equatorial ocean to periodic forcing. *J. Mar. Res., 39, 651–693*, 1981.